Dynamic universality class of model H with frustrated diffusion: ϵ expansion

Ho-Ung Yee*

Department of Physics, University of Illinois, Chicago, Illinois 60607, USA
and RIKEN-BNL Research Center, Brookhaven National Laboratory, Upton, New York 11973-5000, USA

(Received 15 August 2017; published 8 January 2018)

We study a variation of the dynamic universality class of model H in a spatial dimension of $d = 4 - \epsilon$, by frustrating charge diffusion and momentum density fluctuations along $d_T = 1$ or $d_T = 2$ dimensions, while keeping the same dynamics of model H in the other $d_L = d - d_T$ dimensions. The case of $d_T = 2$ describes the QCD critical point in a background magnetic field. We find that these models belong to a different dynamical universality class due to extended conservation laws compared to the model H, although the static universality class remains the same as the 3-dimensional Ising model. We compute the dynamic critical exponents of these models in first order of ϵ-expansion to find that $x_\lambda \approx 0.847\epsilon$, $x_{\bar{\eta}} \approx 0.153\epsilon$, and $z = 4 - x_\lambda \approx 3.15$ when $\epsilon = 1$ and $d_T = 2$. For $d_T = 1$ the results are numerically similar to the model H values: $z \approx 3.08$.

DOI: 10.1103/PhysRevD.97.016003

I. INTRODUCTION

Critical phenomena near phase transitions are often characterized by universality classes. In the critical regime, the correlation length of fluctuations becomes macroscopically large compared to microscopic scales, and the governing dynamics is insensitive to microscopic details, except certain global features such as symmetries and dimensions (equivalently, phase space volumes). This universality allows us to study the key features of critical phenomena in many different systems in terms of a few simple prototypical models that describe each universality class. If one is interested in the static equilibrium thermodynamic critical phenomena, it is enough to specify the model in terms of its free energy functional on the appropriate set of its order parameters. However, the critical phenomena may also appear in how the system responds to time-dependent perturbations or in how fast the system approaches to its thermal equilibrium when it starts from off-equilibrium conditions that are not too far from equilibrium. The dynamic universality classes aim to characterize these real-time critical phenomena in terms of simple prototypical stochastic real-time models. The dynamic universality classes are built on top of the static universality classes, and in principle, two systems with a common static universality class may belong to different dynamic universality classes. Some of the main divisors in this classification are whether an order parameter is conserved, and whether two dynamic variables are coupled nonlinearly with each other.

One of the dynamic universality classes is the "model H" [1,2], which describes the critical dynamics of a gas-liquid critical point. The model H has two dynamical fields: a conserved charge density (which is the order parameter of the static universality class, the 3D Ising class) and the shear component of momentum density fluctuations. Their dynamics in long wave-lengths near the critical regime is mainly governed by diffusion dynamics due to their conservation laws. What gives a nontrivial infrared (IR) dynamics in the model H is a nonlinear coupling between these two diffusion dynamics [3,4]. A simple way of looking at this coupling is the following: in the presence of both charge density ψ and the momentum fluctuations $\boldsymbol{j}$, there naturally appears a charge flow due to convection $\psi\boldsymbol{j}$, which in turn affects the conservation dynamics of the charge density ψ. See for example Ref. [2] for a more intuitive discussion why this coupling may affect the infrared critical dynamics in a non-trivial way.

The model H has been studied in the ϵ-expansion in Ref. [1], generalizing the technique used in static critical phenomena [5,6]. The dimensionless coupling constant responsible for the nonlinear coupling between the charge density and momentum fluctuations has an IR fixed point of order ϵ, and a perturbation theory in terms of ϵ-expansion is possible. The conductivity λ and the shear viscosity $\bar{\eta}$ defined in the hydrodynamic regime of $k < \xi^{-1}$ (k refers to the inverse length scale, and ξ is the correlation length) diverge as $\lambda \sim \xi^{x_\lambda}$ and $\bar{\eta} \sim \xi^{x_\eta}$ with the critical exponents x_λ and x_η. In the critical (or scaling) regime $k > \xi^{-1}$ on the

*hyee@uic.edu

other hand, the slowest relaxation mode ("critical slowing-down") turns out to be the charge diffusion mode which has the scaling form of dispersion relation $\omega \sim -ik^z$ that defines the dynamic critical exponent z. The results for dynamical critical exponents such as x_λ, x_η and z are available up to ϵ^2 [1]. When $\epsilon = 1$, they are numerically $x_\lambda \approx 1$, $x_\eta \approx 0$ and $z \approx 3$.

It has been argued that the model H describes the dynamic universality class of a possible critical point in quantum chromodynamics (QCD) with finite temperature and baryon density [7–9]. The conserved order parameter in this case comes from a linear combination of baryon charge and energy density. Although there has not been an experimental confirmation on the existence of the QCD critical point, there are tantalizing signals of baryon number cumulants observed in relativistic heavy-ion collision experiments in Relativistic Heavy-Ion Colliders (RHIC) [10], which seem to be consistent with what one would expect from the static universality class of 3D Ising model [11]. However, to draw more reliable conclusions from these encouraging results, we have to take into account that the quark-gluon plasma fireball created in such experiments is of finite size, and moreover it expands in time, which drives the system off-equilibrium. Even if the system's instantaneous parameters are on the critical point, the correlation length will develop in a finite time [8], and the detailed knowledge on the dynamic universality class is crucial to study how the system, in particular the cumulants observables, changes in real-time in the experiments [12]. One of the important parameters is the dynamic critical exponent z that characterizes the critical slowing-down time scale of the system.

In relativistic heavy-ion collisions with a finite impact parameter, there exists a huge, albeit transient, magnetic field produced by two relativistic, heavy-charged projectiles colliding together, and the quark-gluon plasma created in such experiments may be subject to this magnetic field whose strength could be as large as 10^{18} Gauss (100 times stronger than the strongest magnetic field in the Universe in "magnetars") [13,14]. Although the lifetime of this magnetic field is short and the strength quickly drops to one hundreds of its original value and stays almost constant due to conductivity of the plasma [15,16], it is still interesting to study its possible effect on the critical dynamics of QCD.

One of the major effects from the strong magnetic field to the real-time dynamics of charge density and momentum fluctuations is that the momentum fluctuations in perpendicular directions to the magnetic field are damped with a finite relaxation time and are no longer relevant slow critical variables [17]. To see this more explicitly, let us start from the fluid equations of motion of the plasma with a background magnetic field along $z = x^3$ direction (that is, $F_{12} = B$),

$$J^\mu = \lambda F^{\mu\nu} u_\nu, \qquad \partial_\mu T^{\mu\nu} = F^{\nu\alpha} J_\alpha, \tag{1.1}$$

where J^μ is the charge current, $T^{\mu\nu} = w u^\mu u^\nu + p\eta^{\mu\nu}$ is the energy-momentum, u^μ is the fluid velocity field and λ is the conductivity. For small transverse velocity v_1, v_2, the first equation gives the current $J^i = \lambda B \epsilon^{ij} v_j$ ($i, j = 1, 2$). In the homogeneous limit ($\boldsymbol{k} \to 0$), the second equation gives

$$\partial_t v_i = -\frac{\lambda B^2}{w} v_i \equiv -\frac{1}{\tau_R} v_i, \tag{1.2}$$

so that $v_{1,2}$ has a finite relaxation time τ_R in $\boldsymbol{k} \to 0$ limit, that is, it is not a slow critical variable. Once we remove $v_{1,2}$ (equivalently, momentum fluctuations along 1,2 directions) from the critical dynamical modes, there is no nonlinear coupling between the momentum and charge density that gives renormalization for the transverse conductivity along (1,2) directions: the physical transverse conductivity remains finite in infrared. Note that the conductivity appearing in (1.2) is the transverse conductivity. The naive scaling dimension of the conductivity is negative when $z < 4$ [see (3.3)] and the transverse conductivity therefore becomes irrelevant in the infrared in the renormalization group. On the other hand, the physical conductivity along the remaining longitudinal direction will be shown to diverge near the critical point due to the nonlinear coupling, and its renormalized value goes to a finite fixed point in the renormalization group (see the discussion in Sec. IV).

Motivated by this, we study a particular variation of dynamic universality class of model H in the ϵ-expansion: we will frustrate the charge conductivity and the momentum density fluctuations along $d_T = 1$ or $d_T = 2$ spatial dimensions (denoted as $\boldsymbol{x}_T$), while keeping them in the rest $d_L = 4 - d_T - \epsilon$ dimensions (denoted as $\boldsymbol{x}_\parallel$). The $d_T = 2$ case should describe the dynamic universality class for the QCD critical point in a background magnetic field as discussed in the above. The case of $d_T = 1$ is more of pure theoretical interests, but it may have some application in layered condensed matter systems where diffusion along one direction is frustrated. We will find that these variations of model H belong to dynamic universality classes that are different from the original model H, and the dynamic critical exponents such as x_λ, x_η and z are different: we compute these exponents in first order of the ϵ-expansion by using the Wilsonian renormalization group method [5,6]. Using the Feynman diagram method of Ref. [18] one can in principle continue to higher orders in ϵ. The reason why we get the different dynamic universality classes in these models is that the symmetries are enlarged from those of the original model H. In the absence of charge diffusion along d_T, the integrated charge density along d_L at any given point in d_T is conserved: the symmetry group is infinite dimensional.

Despite that the real-time dynamics in these models breaks rotational symmetry, we assume that the static universality class remains to be the isotropic 3D Ising model described by a theory of a scalar field ψ with quartic interaction. This is reasonable since the only relevant or marginal perturbation near critical regime that breaks rotational symmetry is of a form $K^{ij}\partial_i\psi\partial_j\psi$ and we can make it isotropic by diagonalizing and rescaling the coordinates.

II. DESCRIPTION OF THE MODEL

We will follow the notations in Refs. [1,2], and denote a conserved order parameter by ψ and the momentum density vector by $\boldsymbol{j}_\parallel$ which has components only along the space $\boldsymbol{x}_\parallel$ of dimension $d_L = 4-\epsilon-d_T$ in our model. The static equilibrium thermal distribution is given by $e^{-F[\psi,\boldsymbol{j}_\parallel]}$ where F is the free energy functional of 3D Ising universality class

$$F = \int d^{4-\epsilon}x\left(\frac{1}{2}(\partial\psi)^2 + \frac{r\Lambda^2}{2}\psi^2 + \frac{u\Lambda^\epsilon}{4!}\psi^4 + \frac{1}{2}\boldsymbol{j}_\parallel\cdot\boldsymbol{j}_\parallel\right), \tag{2.1}$$

where Λ is the physical UV-cutoff in momentum space. Writing the parameters of the model in the above way, (r,u) are dimensionless. The dynamical model is a simple twist of the model H with frustrated diffusion along $\boldsymbol{x}_T$,

$$\frac{\partial\psi}{\partial t} = \lambda_\parallel\Lambda^{z-4}\nabla_\parallel^2\frac{\delta F}{\delta\psi} - g\Lambda^{z-3+\epsilon/2}\boldsymbol{\nabla}_\parallel\psi\cdot\frac{\delta F}{\delta\boldsymbol{j}_\parallel} + \theta, \tag{2.2}$$

$$\frac{\partial\boldsymbol{j}_\parallel}{\partial t} = \mathcal{P}\left(\bar\eta_\perp\Lambda^{z-2}\nabla_\perp^2\boldsymbol{j}_\parallel + \bar\eta_\parallel\Lambda^{z-2}\nabla_\parallel^2\boldsymbol{j}_\parallel + g\Lambda^{z-3+\epsilon/2}\boldsymbol{\nabla}_\parallel\psi\frac{\delta F}{\delta\psi} + \boldsymbol{\xi}\right), \tag{2.3}$$

where $\mathcal{P}$ projects the vector components onto the subspace perpendicular to a momentum vector $\boldsymbol{k}$ in Fourier space, that is, it keeps only the shear components. Since $\boldsymbol{j}_\parallel$ is already perpendicular to $\boldsymbol{k}_\perp$, it is practically a projection operator in $\boldsymbol{x}_\parallel$ space;

$$\mathcal{P}\to\delta_\parallel^{ij} - \frac{\boldsymbol{k}_\parallel^i\boldsymbol{k}_\parallel^j}{\boldsymbol{k}_\parallel^2}. \tag{2.4}$$

The random noises $(\theta,\boldsymbol{\xi})$ are Gaussian with the strength determined by Fluctuation-Dissipation relation,

$$\begin{aligned}\langle\theta(\boldsymbol{x},t)\theta(\boldsymbol{x}',t')\rangle &= -2\lambda_\parallel\Lambda^{z-4}\nabla_\parallel^2\delta(\boldsymbol{x}-\boldsymbol{x}')\delta(t-t'),\\ \langle\boldsymbol{\xi}^i(\boldsymbol{x},t)\boldsymbol{\xi}^j(\boldsymbol{x}',t')\rangle &= -2\delta^{ij}(\eta_\perp\Lambda^{z-2}\nabla_\perp^2 + \bar\eta_\parallel\Lambda^{z-2}\nabla_\parallel^2)\delta(\boldsymbol{x}-\boldsymbol{x}')\delta(t-t'),\end{aligned} \tag{2.5}$$

which ensures that the equilibrium distribution is e^{-F}. The $\lambda_\parallel$ is the conductivity, $\bar\eta_{\parallel,\perp}$ are the shear viscosities in $\boldsymbol{x}_\parallel$ and $\boldsymbol{x}_\perp$ spaces respectively, which are in general different. We will see that their values at the IR fixed point are indeed different, but comparable to each other so we need to keep them both. The g is the nonlinear coupling between two dynamical modes in model H, which drives a nontrivial IR fixed point. The exponent z is the scale dimension of the frequency ω relative to the momentum $\boldsymbol{k}$. All parameters defined as above are then dimensionless.

Although we can perform the Wilsonian renormalization group at the level of the above equations of motion, we choose to work in a language of stochastic field theory or a path integral, where the renormalization procedure looks more organized (at least to the eyes of the author). For that purpose, we introduce the "a-type" fields $(\psi_a,\boldsymbol{j}_{\parallel a})$ and call the original variables in the equations of motion the "r-type" fields $(\psi_r,\boldsymbol{j}_{\parallel r})$, then consider a path integral of e^S with an action $S=\int dt\int d^{4-\epsilon}x\mathcal{L}$,

$$\begin{aligned}\mathcal{L} = {}& i\psi_a\left(\frac{\partial\psi_r}{\partial t} - \lambda_\parallel\Lambda^{z-4}\nabla_\parallel^2\frac{\delta F}{\delta\psi_r} + g\Lambda^{z-3+\epsilon/2}\boldsymbol{\nabla}_\parallel\psi_r\cdot\frac{\delta F}{\delta\boldsymbol{j}_{\parallel r}} - \theta\right)\\ &+ i\boldsymbol{j}_{\parallel a}\cdot\mathcal{P}\left(\frac{\partial\boldsymbol{j}_{\parallel r}}{\partial t} - \bar\eta_\perp\Lambda^{z-2}\nabla_\perp^2\boldsymbol{j}_{\parallel r} - \bar\eta_\parallel\Lambda^{z-2}\nabla_\parallel^2\boldsymbol{j}_{\parallel r}\right.\\ &\left. - g\Lambda^{z-3+\epsilon/2}\boldsymbol{\nabla}_\parallel\psi_r\frac{\delta F}{\delta\psi_r} - \boldsymbol{\xi}\right) - \frac{1}{2}\theta\frac{1}{-2\lambda_\parallel\Lambda^{z-4}\nabla_\parallel^2}\theta\\ &- \frac{1}{2}\boldsymbol{\xi}\cdot\frac{\mathcal{P}}{-2(\eta_\perp\Lambda^{z-2}\nabla_\perp^2 + \bar\eta_\parallel\Lambda^{z-2}\nabla_\parallel^2)}\boldsymbol{\xi}.\end{aligned} \tag{2.6}$$

The correspondence to the usual (r,a)-fields in the Schwinger-Keldysh formalism is clear: the "r-type" fields are classical variables. The path integral over the "a-type" field localizes the path integral of "r-type" fields to the solutions of the original stochastic Langevin equations of motion with the Gaussian random noises $(\theta,\boldsymbol{\xi})$. The "wave function" at time t is precisely then the probability distribution of the classical variables at time t generated by solutions of the stochastic equations of motion.

We can integrate out the noise variables $(\theta,\boldsymbol{\xi})$ as they are Gaussian to obtain

$$\begin{aligned}\mathcal{L}' = {}& i\psi_a\left(\frac{\partial\psi_r}{\partial t} - \lambda_\parallel\Lambda^{z-4}\nabla_\parallel^2\frac{\delta F}{\delta\psi_r} + g\Lambda^{z-3+\epsilon/2}\boldsymbol{\nabla}_\parallel\psi_r\cdot\frac{\delta F}{\delta\boldsymbol{j}_{\parallel r}}\right)\\ &+ i\boldsymbol{j}_{\parallel a}\cdot\mathcal{P}\left(\frac{\partial\boldsymbol{j}_{\parallel r}}{\partial t} - \bar\eta_\perp\Lambda^{z-2}\nabla_\perp^2\boldsymbol{j}_{\parallel r} - \bar\eta_\parallel\Lambda^{z-2}\nabla_\parallel^2\boldsymbol{j}_{\parallel r}\right.\\ &\left. - g\Lambda^{z-3+\epsilon/2}\boldsymbol{\nabla}_\parallel\psi_r\frac{\delta F}{\delta\psi_r}\right) + \lambda_\parallel\Lambda^{z-4}\psi_a\nabla_\parallel^2\psi_a\\ &+ \boldsymbol{j}_{\parallel a}\cdot(\bar\eta_\perp\Lambda^{z-2}\nabla_\perp^2 + \bar\eta_\parallel\Lambda^{z-2}\nabla_\parallel^2)\mathcal{P}\boldsymbol{j}_{\parallel a}.\end{aligned} \tag{2.7}$$

Upon "quantization" the "a-type" fields are canonical conjugate to the "r-type" fields: $\psi_a\sim i\frac{\partial}{\partial\psi_r}$. The "Schrödinger equation" is the Fokker-Planck equation.

What we do in this formulation corresponds to the renormalization in terms of the Fokker-Planck equation, instead of the original stochastic equations of motion. Obviously they should be equivalent.

III. RENORMALIZATION GROUP IN ϵ-EXPANSION

We follow the standard procedure (see Refs. [1,5,6]) of thinning the momentum shell around the cutoff Λ, and integrate over the shell

$$\Lambda/b < |\boldsymbol{k}| < \Lambda, \tag{3.1}$$

with a constant $b > 1$ close to 1. After this we rescale the coordinates or equivalently the momenta to get back to the same cutoff Λ in the rescaled momentum space $\boldsymbol{k}'$;

$$\begin{aligned} \boldsymbol{k}' &= b\boldsymbol{k}, \\ \omega' &= b^z\omega. \end{aligned} \tag{3.2}$$

Without the nonlinear couplings such as g and u, the parameters of the theory would change at each step simply by their naive scaling dimensions:

$$\begin{aligned} \lambda_\parallel' &= b^{z-4}\lambda_\parallel \approx \lambda_\parallel + (z-4)\lambda_\parallel \log b, \\ (\bar\eta_\perp', \bar\eta_\parallel') &= b^{z-2}(\bar\eta_\perp, \bar\eta_\parallel) \approx (\bar\eta_\perp, \bar\eta_\parallel) + (z-2)(\bar\eta_\perp, \bar\eta_\parallel)\log b, \\ g' &= b^{z-3+\epsilon/2} g \approx g + (z-3+\epsilon/2) g \log b. \end{aligned} \tag{3.3}$$

There are similar equations for the static parameters (r, u). The nonlinear couplings by (u, g) give rise to additional contributions to the above. These are what we need to compute.

In the critical regime, the IR cutoff set by the correlation length $\Lambda_{\rm IR} \sim \xi^{-1}$ is far separated from the UV cutoff Λ. After N steps of the above procedure where $b^N\xi^{-1} = \Lambda$, the UV and IR cutoffs in the renormalized theory become comparable and the scaling behavior is lost. This is the point where the hydrodynamic regime sets in, and the renormalization group running of the parameters of the theory stops and further contributions to these parameters are IR-finite. The number of steps of the above procedure to be performed to reach this is $N = \log(\Lambda\xi)/\log b$. The renormalized parameter r starts close to its fixed point value which is of order $r^* \sim \epsilon$, and we can neglect it in the propagator in the leading order perturbation in ϵ. In each step of the above procedure, the deviation of the renormalized r from r^* grows, and only after performing the same $N = \log(\Lambda\xi)/\log b$ steps it becomes of order 1: this is because the scaling behavior is lost precisely when the renormalized r deviates from $r^* \sim \epsilon$ by order 1. Therefore r stays of order ϵ in most of the N-steps, and we can neglect $r \ll 1$ in the propagators in all N-steps in the leading perturbation in ϵ-expansion [5,6].

When $z > 1$, the cutoff in frequency space can be taken to be infinite. Even if we started with a same cutoff Λ in the frequency space, a step of above procedure would change it to $b^{z-1}\Lambda$. In the critical regime where $N \gg 1$, this cutoff quickly becomes much larger than Λ in most of the N steps.

The observed physical parameters of the theory are the ones without rescaling the coordinates and the time: they are the parameters measured in terms of the original coordinates and time. The effect of rescaling coordinates for them is simply given by (3.3), and therefore the observed physical parameters are obtained from the renormalized parameters by undoing the naive scaling transformation (3.3) [1,5,6]:

$$\begin{aligned} \lambda_\parallel^{\rm phys} &= (b^{4-z})^N \lambda_\parallel^*, \\ (\bar\eta_\perp^{\rm phys}, \bar\eta_\parallel^{\rm phys}) &= (b^{2-z})^N (\bar\eta_\perp^*, \bar\eta_\parallel^*), \\ g^{\rm phys} &= (b^{3-z-\epsilon/2})^N g^*, \end{aligned} \tag{3.4}$$

where the starred parameters are the renormalized parameters after performing the large N-steps (they could be a finite fixed point value or not). In effect, the physical parameters in the above capture only the contributions from the nonlinear couplings in the relevant momentum range $\xi^{-1} < |\boldsymbol{k}| < \Lambda$ as they should.

With these general discussions reviewed, we now compute the contributions from the nonlinear couplings (g, u) to the renormalization group equation. We can apply perturbation theory in these couplings since their fixed point values will be of order ϵ. After integrating over the momentum shell, the action $S + \delta S$ with a new cutoff Λ/b is expected to be given by a new set of parameters

$$(\lambda_\parallel, \bar\eta_{\perp,\parallel}) \to (\lambda_\parallel + \delta\lambda_\parallel, \bar\eta_{\perp,\parallel} + \delta\bar\eta_{\perp,\parallel}), \qquad F \to F + \delta F. \tag{3.5}$$

The contribution to g will be shown to be absent. The contributions from the nonlinear couplings $(\delta\lambda_\parallel, \delta\bar\eta_{\perp,\parallel}, \delta F)$ are of first order in $\log b$ in small $\log b$ limit. The effect of rescaling (3.3) to restore the original cutoff Λ and the above nonlinear contribution are therefore additive to each other to first order in $\log b$.

First, the δF should be identical to what one would have in a static renormalization group [1], because the equilibrium distribution after integrating over the momentum shell is $e^{-(F+\delta F)}$ by the fluctuation-dissipation relation, and this must agree with what one would have in a static renormalization after integrating over the same momentum shell. Although this is guaranteed by the fluctuation-dissipation relation in the original unintegrated theory, it is assuring to see this explicitly for a few lowest order contributions, which we have checked. From the known static renormalization group [5,6], we have

$$\begin{aligned} F + \delta F = \int d^{4-\epsilon}x \Big(& (1 + \eta \log b)\frac{1}{2}(\partial\psi)^2 + \frac{1}{2}(r + \delta r)\Lambda^2\psi^2 \\ & + \frac{1}{4!}(u + \delta u)\Lambda^\epsilon \psi^4 \Big), \end{aligned} \tag{3.6}$$

where $\eta/2 \sim \epsilon^2$ is the anomalous dimension of ψ, and the other terms are not of our interest for the renormalization of the transport coefficients ($r + \delta r$ for example is order ϵ in the scaling regime and will be neglected in the propagator).

Looking at how F appears in the charge diffusion term in the action (2.7), this wave-function renormalization contributes to $\delta\lambda_\parallel$ as

$$\delta\lambda_\parallel = \eta\lambda_\parallel \log b. \tag{3.7}$$

The other leading contributions to $(\delta\lambda_\parallel, \delta\bar{\eta}_{\perp,\parallel})$ come from the coupling g. One can compute these by looking at the contributions to the $\psi_a\psi_r$ and $\boldsymbol{j}_{\parallel a}\boldsymbol{j}_{\parallel r}$ terms in the action as they contain these transport coefficients. The real-time Feynman diagrams generating a $\psi_a\psi_r$ term in δS are shown in Fig. 1. There are two real-time diagrams to be summed. In Fig. 2 we show the real-time diagram generating a $\boldsymbol{j}_{\parallel a}\boldsymbol{j}_{\parallel r}$ term in δS. The solid lines are the propagators of ψ-field and the wavy lines are for the $\boldsymbol{j}_\parallel$-fields. These propagators are easily found from the quadratic part of the action S to be

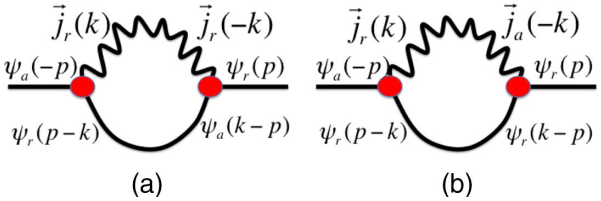

FIG. 1. The two real-time diagrams for renormalization of $\lambda_\parallel$.

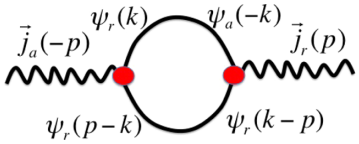

FIG. 2. The real-time diagram for renormalization of $\bar{\eta}_\perp$ and $\bar{\eta}_\parallel$.

$$\begin{aligned}
&\langle\psi_r(k)\psi_a(-k)\rangle = \langle\psi_a(k)\psi_r(-k)\rangle^* = \frac{1}{-\omega - i\lambda_\parallel\Lambda^{z-4}\boldsymbol{k}_\parallel^2\boldsymbol{k}^2},\\
&\langle\psi_r(k)\psi_r(-k)\rangle = \frac{2\lambda_\parallel\Lambda^{z-4}\boldsymbol{k}_\parallel^2}{\omega^2 + (\lambda_\parallel\Lambda^{z-4}\boldsymbol{k}_\parallel^2\boldsymbol{k}^2)^2}, \qquad \langle\psi_a(k)\psi_a(-k)\rangle = 0,\\
&\langle\boldsymbol{j}^i_{\parallel r}(k)\boldsymbol{j}^j_{\parallel a}(-k)\rangle = \langle\boldsymbol{j}^i_{\parallel a}(k)\boldsymbol{j}^j_{\parallel r}(-k)\rangle^* = \frac{(\delta^{ij}_\parallel - \frac{\boldsymbol{k}^i_\parallel\boldsymbol{k}^j_\parallel}{\boldsymbol{k}^2_\parallel})}{-i\omega - i(\bar{\eta}_\perp\Lambda^{z-2}\boldsymbol{k}^2_\perp + \bar{\eta}_\parallel\Lambda^{z-2}\boldsymbol{k}^2_\parallel)},\\
&\langle\boldsymbol{j}^i_{\parallel r}(k)\boldsymbol{j}^j_{\parallel r}(-k)\rangle = \frac{2(\bar{\eta}_\perp\Lambda^{z-2}\boldsymbol{k}^2_\perp + \bar{\eta}_\parallel\Lambda^{z-2}\boldsymbol{k}^2_\parallel)(\delta^{ij}_\parallel - \frac{\boldsymbol{k}^i_\parallel\boldsymbol{k}^j_\parallel}{\boldsymbol{k}^2_\parallel})}{\omega^2 + (\bar{\eta}_\perp\Lambda^{z-2}\boldsymbol{k}^2_\perp + \bar{\eta}_\parallel\Lambda^{z-2}\boldsymbol{k}^2_\parallel)^2}, \qquad \langle\boldsymbol{j}^i_{\parallel a}(k)\boldsymbol{j}^j_{\parallel a}(-k)\rangle = 0,
\end{aligned} \tag{3.8}$$

where $k = (\omega, \boldsymbol{k}) = (\omega, \boldsymbol{k}_\parallel, \boldsymbol{k}_\perp)$ is a frequency-momentum in Fourier space. Each vertex in the diagrams is from the g coupling in the action, which is

$$ig\Lambda^{z-3+\epsilon/2}\psi_a\boldsymbol{\nabla}_\parallel\psi_r\cdot\boldsymbol{j}_{\parallel r} - ig\Lambda^{z-3+\epsilon/2}\boldsymbol{j}_{\parallel a}\cdot\boldsymbol{\nabla}_\parallel\psi_r(-\nabla^2\psi_r). \tag{3.9}$$

We first write down the expression for the first diagram in Fig. 1.

$$-g^2\Lambda^{2z-6+\epsilon}\int_p\psi_a(-p)\psi_r(p)\int_k\frac{i(\boldsymbol{p}^i_\parallel - \boldsymbol{k}^i_\parallel)i\boldsymbol{p}^j_\parallel}{-(\Omega-\omega) - i\lambda_\parallel\Lambda^{z-4}(\boldsymbol{p}_\parallel - \boldsymbol{k}_\parallel)^2(\boldsymbol{p}-\boldsymbol{k})^2}\times\frac{2(\bar{\eta}_\perp\Lambda^{z-2}\boldsymbol{k}^2_\perp + \bar{\eta}_\parallel\Lambda^{z-2}\boldsymbol{k}^2_\parallel)(\delta^{ij}_\parallel - \frac{\boldsymbol{k}^i_\parallel\boldsymbol{k}^j_\parallel}{\boldsymbol{k}^2_\parallel})}{\omega^2 + (\bar{\eta}_\perp\Lambda^{z-2}\boldsymbol{k}^2_\perp + \bar{\eta}_\parallel\Lambda^{z-2}\boldsymbol{k}^2_\parallel)^2}, \tag{3.10}$$

where $p = (\Omega, \boldsymbol{p})$ is the external momentum, and we denote

$$\int_p = \int\frac{d\Omega}{2\pi}\int_{\boldsymbol{p}} = \int\frac{d\Omega}{2\pi}\int\frac{d^{4-\epsilon}\boldsymbol{p}}{(2\pi)^{4-\epsilon}}, \tag{3.11}$$

so that $\int_p\psi_a(-p)\psi_r(p) = \int dt\int d^{4-\epsilon}\boldsymbol{x}\psi_a(x)\psi_r(x)$. Computing ω integration by closing the contour in the lower half-plane, we obtain

$$+ig^2\Lambda^{2z-6+\epsilon}\int_p\psi_a(-p)\psi_r(p)\boldsymbol{p}^2_\parallel\int_k\frac{(1-\frac{(\boldsymbol{k}_\parallel\cdot\boldsymbol{p}_\parallel)^2}{\boldsymbol{k}^2_\parallel\boldsymbol{p}^2_\parallel})}{-i\Omega + (\bar{\eta}_\perp\Lambda^{z-2}\boldsymbol{k}^2_\perp + \bar{\eta}_\parallel\Lambda^{z-2}\boldsymbol{k}^2_\parallel) + \lambda_\parallel\Lambda^{z-4}(\boldsymbol{k}_\parallel - \boldsymbol{p}_\parallel)^2(\boldsymbol{k}-\boldsymbol{p})^2}, \tag{3.12}$$

where $\boldsymbol{k}$ integration to be performed in the momentum shell $\Lambda/b < |\boldsymbol{k}| < \Lambda$. The second diagram in Fig. 1 is similarly computed to be

$$g^2\Lambda^{2z-6+\epsilon}\int_p \psi_a(-p)\psi_r(p)\int_k \frac{i(\boldsymbol{p}_\parallel^i-\boldsymbol{k}_\parallel^i)i(\boldsymbol{p}_\parallel^j(\boldsymbol{k}-\boldsymbol{p})^2+(\boldsymbol{k}_\parallel^j-\boldsymbol{p}_\parallel^j)\boldsymbol{p}^2)}{(\omega-\Omega)^2+(\lambda_\parallel\Lambda^{z-4}(\boldsymbol{p}_\parallel-\boldsymbol{k}_\parallel)^2(\boldsymbol{p}-\boldsymbol{k})^2)^2}\times\frac{2\lambda_\parallel\Lambda^{z-4}(\boldsymbol{k}_\parallel-\boldsymbol{p}_\parallel)^2(\delta_\parallel^{ij}-\frac{\boldsymbol{k}_\parallel^i\boldsymbol{k}_\parallel^j}{\boldsymbol{k}_\parallel^2})}{-\omega-i(\bar\eta_\perp\Lambda^{z-2}\boldsymbol{k}_\perp^2+\bar\eta_\parallel\Lambda^{z-2}\boldsymbol{k}_\parallel^2)}$$
$$=-ig^2\Lambda^{2z-6+\epsilon}\int_p\psi_a(-p)\psi_r(p)\boldsymbol{p}_\parallel^2\int_k\frac{(1-\frac{(\boldsymbol{k}_\parallel\cdot\boldsymbol{p}_\parallel)^2}{\boldsymbol{k}_\parallel^2\boldsymbol{p}_\parallel^2})(1-\frac{\boldsymbol{p}^2}{(\boldsymbol{k}-\boldsymbol{p})^2})}{-i\Omega+(\bar\eta_\perp\Lambda^{z-2}\boldsymbol{k}_\perp^2+\bar\eta_\parallel\Lambda^{z-2}\boldsymbol{k}_\parallel^2)+\lambda_\parallel\Lambda^{z-4}(\boldsymbol{k}_\parallel-\boldsymbol{p}_\parallel)^2(\boldsymbol{k}-\boldsymbol{p})^2}, \tag{3.13}$$

and the sum of the two becomes

$$+ig^2\Lambda^{2z-6+\epsilon}\int_p\psi_a(-p)\psi_r(p)\boldsymbol{p}_\parallel^2\boldsymbol{p}^2\int_k\frac{(1-\frac{(\boldsymbol{k}_\parallel\cdot\boldsymbol{p}_\parallel)^2}{\boldsymbol{k}_\parallel^2\boldsymbol{p}_\parallel^2})}{[(\bar\eta_\perp\Lambda^{z-2}\boldsymbol{k}_\perp^2+\bar\eta_\parallel\Lambda^{z-2}\boldsymbol{k}_\parallel^2)+\lambda_\parallel\Lambda^{z-4}\boldsymbol{k}_\parallel^2\boldsymbol{k}^2]\boldsymbol{k}^2}, \tag{3.14}$$

where we take a limit of a small external momentum compared to the loop momentum: $p \ll k$.

Here comes an important step of approximation in the model H which is self-consistent. We will see that $\bar\eta_{\perp,\parallel}$ grows large in the renormalization group running, while $\lambda_\parallel$ approaches a finite fixed point in the IR: after many steps of renormalization we have $\bar\eta_{\perp,\parallel} \gg \lambda_\parallel$. Since the loop momentum $\boldsymbol{k}$ in the shell is near the cutoff Λ, the term with $\lambda_\parallel$ in the denominator is then negligible compared to the terms with $\bar\eta_{\perp,\parallel}$. This gives finally the expression

$$+ig^2\Lambda^{z-4+\epsilon}\int_p\psi_a(-p)\psi_r(p)\boldsymbol{p}_\parallel^2\boldsymbol{p}^2\int_k\frac{(1-\frac{(\boldsymbol{k}_\parallel\cdot\boldsymbol{p}_\parallel)^2}{\boldsymbol{k}_\parallel^2\boldsymbol{p}_\parallel^2})}{[(\bar\eta_\perp\boldsymbol{k}_\perp^2+\bar\eta_\parallel\boldsymbol{k}_\parallel^2)]\boldsymbol{k}^2}. \tag{3.15}$$

We now describe the $\boldsymbol{k}$ integral in the above. We have

$$\int_k=\frac{1}{(2\pi)^{4-\epsilon}}\int_{\Lambda/b}^{\Lambda}d|\boldsymbol{k}||\boldsymbol{k}|^{3-\epsilon}\int_{S^{3-\epsilon}}d\Omega, \tag{3.16}$$

and the integrand in (3.15) is of a form

$$\frac{1}{|\boldsymbol{k}|^4}F(\Omega), \tag{3.17}$$

with an angular function on the sphere $F(\Omega)$. The $|\boldsymbol{k}|$ integral gives

$$\int_{\Lambda/b}^{\Lambda}\frac{d|\boldsymbol{k}|}{|\boldsymbol{k}|}|\boldsymbol{k}|^{-\epsilon}=\Lambda^{-\epsilon}\log b+\mathcal{O}(\epsilon), \tag{3.18}$$

and in the leading order in ϵ-expansion, the angular integral can be performed in $\epsilon=0$ limit, that is, on the S^3 sphere. We parametrize the $\boldsymbol{k}$ space in this limit as

$$\begin{aligned}\boldsymbol{k}_1&=|\boldsymbol{k}|\cos\theta,\\ \boldsymbol{k}_2&=|\boldsymbol{k}|\sin\theta\cos\phi,\\ \boldsymbol{k}_3&=|\boldsymbol{k}|\sin\theta\sin\phi\cos\chi,\\ \boldsymbol{k}_4&=|\boldsymbol{k}|\sin\theta\sin\phi\sin\chi,\end{aligned} \tag{3.19}$$

with $0<(\theta,\phi)<\pi$ and $0<\chi<2\pi$, and the measure is

$$d\Omega=\sin^2\theta\sin\phi d\theta d\phi d\chi. \tag{3.20}$$

The result of the angular integral depends on the dimension of the $\boldsymbol{x}_T$ space, that is, $d_T=1$ or 2. For $d_T=1$, let us take $\boldsymbol{k}_\perp=\boldsymbol{k}_1$ and $\boldsymbol{k}_\parallel=(\boldsymbol{k}_2,\boldsymbol{k}_3,\boldsymbol{k}_4)$, and let $\boldsymbol{p}_\parallel$ point to $\boldsymbol{k}_4$ direction. The $F(\Omega)$ in this case is

$$F(\Omega,\bar\eta_\perp,\bar\eta_\parallel)=\frac{1-\sin^2\phi\sin^2\chi}{\bar\eta_\perp\cos^2\theta+\bar\eta_\parallel\sin^2\theta},\quad(d_T=1). \tag{3.21}$$

The result should not depend on these choices as one can check. For $d_T=2$, we choose $\boldsymbol{k}_\perp=(\boldsymbol{k}_1,\boldsymbol{k}_2)$ and $\boldsymbol{k}_\parallel=(\boldsymbol{k}_3,\boldsymbol{k}_4)$, and $\boldsymbol{p}_\parallel$ pointing to the $\boldsymbol{k}_4$ direction. Then $F(\Omega)$ becomes

$$F(\Omega,\bar\eta_\perp,\bar\eta_\parallel)=\frac{\cos^2\chi}{\bar\eta_\perp(\cos^2\theta+\sin^2\theta\cos^2\phi)+\bar\eta_\parallel\sin^2\theta\sin^2\phi},\quad(d_T=2). \tag{3.22}$$

With these the (3.15) becomes at leading order in ϵ

$$+ i\frac{g^2\Lambda^{z-4}}{(2\pi)^4}\int d\Omega F(\Omega,\bar{\eta}_\perp,\bar{\eta}_\parallel)\log b\int_p \psi_a(-p)\psi_r(p)\boldsymbol{p}_\parallel^2\boldsymbol{p}^2$$
$$= \frac{g^2\Lambda^{z-4}}{(2\pi)^4}\int d\Omega F(\Omega,\bar{\eta}_\perp,\bar{\eta}_\parallel)\log b\int dt\int d^{4-\epsilon}\boldsymbol{x}\psi_a(x)(-i\nabla_\parallel^2)(-\nabla^2)\psi_r(x), \tag{3.23}$$

where the last line is a space-time expression. Looking at the diffusion term in the action (2.7), this corresponds to a nonlinear contribution we are looking for

$$\delta\lambda_\parallel = \frac{g^2}{(2\pi)^4}\int d\Omega F(\Omega,\bar{\eta}_\perp,\bar{\eta}_\parallel)\log b. \tag{3.24}$$

We next compute the diagram in Fig. 2 for the renormalization of shear viscosities. We have (neglecting an external frequency)

$$g^2\Lambda^{2z-6+\epsilon}\int_p \boldsymbol{j}^i_{\parallel a}(-p)\boldsymbol{j}^j_{\parallel r}(p)\int_k \frac{i(\boldsymbol{k}^i_\parallel-\boldsymbol{p}^i_\parallel)i(\boldsymbol{k}^j_\parallel(\boldsymbol{p}-\boldsymbol{k})^2+(\boldsymbol{p}^j_\parallel-\boldsymbol{k}^j_\parallel)\boldsymbol{k}^2)2\lambda_\parallel\Lambda^{z-4}(\boldsymbol{p}_\parallel-\boldsymbol{k}_\parallel)^2}{(-\omega-i\lambda_\parallel\Lambda^{z-4}\boldsymbol{k}_\parallel^2\boldsymbol{k}^2)(\omega^2+(\lambda_\parallel\Lambda^{z-4}(\boldsymbol{p}_\parallel-\boldsymbol{k}_\parallel)^2(\boldsymbol{p}-\boldsymbol{k})^2)^2)}, \tag{3.25}$$

and performing the ω-integration, we obtain

$$-i\frac{g^2}{\lambda_\parallel}\Lambda^{z-2+\epsilon}\int_p \boldsymbol{j}^i_{\parallel a}(-p)\boldsymbol{j}^j_{\parallel r}(p)\int_k \frac{\boldsymbol{k}^i_\parallel\boldsymbol{k}^j_\parallel(1-\frac{\boldsymbol{k}^2}{(\boldsymbol{k}-\boldsymbol{p})^2})}{(\boldsymbol{k}_\parallel-\boldsymbol{p}_\parallel)^2(\boldsymbol{k}-\boldsymbol{p})^2+\boldsymbol{k}_\parallel^2\boldsymbol{k}^2}. \tag{3.26}$$

Recall that $\boldsymbol{j}_\parallel(p)$ lies in $\boldsymbol{k}_\parallel$ space, *and* is also perpendicular to $\boldsymbol{p}_\parallel$ (and hence to $\boldsymbol{p}$) inside the $\boldsymbol{k}_\parallel$ space to be a shear component. Therefore we can replace in the numerator

$$\boldsymbol{k}^i_\parallel\boldsymbol{k}^j_\parallel \to \frac{1}{3-d_T-\epsilon}\delta^{ij}_{\parallel\perp}\boldsymbol{k}^2_{\parallel\perp}, \tag{3.27}$$

where $\boldsymbol{k}_{\parallel\perp}$ is the subspace inside $\boldsymbol{k}_\parallel$ perpendicular to $\boldsymbol{p}_\parallel$, and its dimension is $d_L-1=3-d_T-\epsilon$. Also expanding the remaining part of the integrand up to the first relevant leading order,

$$\frac{(1-\frac{\boldsymbol{k}^2}{(\boldsymbol{k}-\boldsymbol{p})^2})}{(\boldsymbol{k}_\parallel-\boldsymbol{p}_\parallel)^2(\boldsymbol{k}-\boldsymbol{p})^2+\boldsymbol{k}_\parallel^2\boldsymbol{k}^2}\approx\frac{1}{2\boldsymbol{k}_\parallel^2\boldsymbol{k}^4}\left(\boldsymbol{p}^2-2\frac{(\boldsymbol{k}_\parallel\cdot\boldsymbol{p}_\parallel)^2}{\boldsymbol{k}_\parallel^2}-6\frac{(\boldsymbol{k}\cdot\boldsymbol{p})^2}{\boldsymbol{k}^2}\right), \tag{3.28}$$

the generated action (3.26) then becomes

$$-i\frac{g^2}{\lambda_\parallel}\Lambda^{z-2+\epsilon}\frac{1}{2(3-d_T-\epsilon)}\int_p \boldsymbol{j}_{\parallel a}(-p)\cdot\boldsymbol{j}_{\parallel r}(p)\int_k\frac{\boldsymbol{k}^2_{\parallel\perp}}{\boldsymbol{k}_\parallel^2\boldsymbol{k}^4}\left(\boldsymbol{p}^2-2\frac{(\boldsymbol{k}_\parallel\cdot\boldsymbol{p}_\parallel)^2}{\boldsymbol{k}_\parallel^2}-6\frac{(\boldsymbol{k}\cdot\boldsymbol{p})^2}{\boldsymbol{k}^2}\right), \tag{3.29}$$

which is logarithmically sensitive to the cutoff. The $\boldsymbol{k}$ integral is done similarly as before. There are two types of terms in the result: a term proportional to $\boldsymbol{p}_\perp^2$ and the other proportional to $\boldsymbol{p}_\parallel^2$. They correspond to a renormalization of $\bar{\eta}_\perp$ and $\bar{\eta}_\parallel$ respectively. The first type of term is

$$-i\frac{g^2}{\lambda_\parallel}\Lambda^{z-2}\frac{1}{2(3-d_T-\epsilon)}\frac{1}{(2\pi)^{4-\epsilon}}\int d\Omega\frac{\boldsymbol{k}^2_{\parallel\perp}}{\boldsymbol{k}_\parallel^2}\left(1-6\frac{(\boldsymbol{k}_\perp\cdot\boldsymbol{p}_\perp)^2}{\boldsymbol{k}^2\boldsymbol{p}_\perp^2}\right)\log b\int_p \boldsymbol{j}_{\parallel a}(-p)\cdot\boldsymbol{j}_{\parallel r}(p)\boldsymbol{p}_\perp^2, \tag{3.30}$$

and the second type is

$$-i\frac{g^2\Lambda^{z-2}}{\lambda_\parallel}\frac{1}{2(3-d_T-\epsilon)}\frac{1}{(2\pi)^{4-\epsilon}}\int d\Omega\frac{\boldsymbol{k}^2_{\parallel\perp}}{\boldsymbol{k}_\parallel^2}\left(1-2\frac{(\boldsymbol{k}_\parallel\cdot\boldsymbol{p}_\parallel)^2}{\boldsymbol{k}_\parallel^2\boldsymbol{p}_\parallel^2}-6\frac{(\boldsymbol{k}_\parallel\cdot\boldsymbol{p}_\parallel)^2}{\boldsymbol{k}^2\boldsymbol{p}_\parallel^2}\right)\log b\int_p \boldsymbol{j}_{\parallel a}(-p)\cdot\boldsymbol{j}_{\parallel r}(p)\boldsymbol{p}_\parallel^2. \tag{3.31}$$

What remains in these terms is an angular integration on S^3 in $\epsilon = 0$ limit. Using the parametrization (3.19), we obtain for $d_T = 1$ case

$$\frac{1}{(2\pi)^4}\int d\Omega \frac{\boldsymbol{k}_{\parallel\perp}^2}{\boldsymbol{k}_\parallel^2}\left(1-6\frac{(\boldsymbol{k}_\perp\cdot\boldsymbol{p}_\perp)^2}{\boldsymbol{k}^2\boldsymbol{p}_\perp^2}\right) = -\frac{1}{8\pi^2}\frac{1}{3},$$
$$\frac{1}{(2\pi)^4}\int d\Omega \frac{\boldsymbol{k}_{\parallel\perp}^2}{\boldsymbol{k}_\parallel^2}\left(1-2\frac{(\boldsymbol{k}_\parallel\cdot\boldsymbol{p}_\parallel)^2}{\boldsymbol{k}_\parallel^2\boldsymbol{p}_\parallel^2}-6\frac{(\boldsymbol{k}_\parallel\cdot\boldsymbol{p}_\parallel)^2}{\boldsymbol{k}^2\boldsymbol{p}_\parallel^2}\right) = -\frac{1}{8\pi^2}\frac{1}{5}, \tag{3.32}$$

and for $d_T = 2$ case,

$$\frac{1}{(2\pi)^4}\int d\Omega \frac{\boldsymbol{k}_{\parallel\perp}^2}{\boldsymbol{k}_\parallel^2}\left(1-6\frac{(\boldsymbol{k}_\perp\cdot\boldsymbol{p}_\perp)^2}{\boldsymbol{k}^2\boldsymbol{p}_\perp^2}\right) = -\frac{1}{8\pi^2}\frac{1}{4},$$
$$\frac{1}{(2\pi)^4}\int d\Omega \frac{\boldsymbol{k}_{\parallel\perp}^2}{\boldsymbol{k}_\parallel^2}\left(1-2\frac{(\boldsymbol{k}_\parallel\cdot\boldsymbol{p}_\parallel)^2}{\boldsymbol{k}_\parallel^2\boldsymbol{p}_\parallel^2}-6\frac{(\boldsymbol{k}_\parallel\cdot\boldsymbol{p}_\parallel)^2}{\boldsymbol{k}^2\boldsymbol{p}_\parallel^2}\right) = -\frac{1}{8\pi^2}\frac{1}{8}. \tag{3.33}$$

From these, we finally obtain the nonlinear contributions to the renormalization of $\bar\eta_\perp$ and $\bar\eta_\parallel$,

$$\delta\bar\eta_\perp = \frac{1}{12}\frac{1}{8\pi^2}\frac{g^2}{\lambda_\parallel}\log b, \qquad \delta\bar\eta_\parallel = \frac{1}{20}\frac{1}{8\pi^2}\frac{g^2}{\lambda_\parallel}\log b, \quad (d_T = 1) \tag{3.34}$$

$$\delta\bar\eta_\perp = \frac{1}{8}\frac{1}{8\pi^2}\frac{g^2}{\lambda_\parallel}\log b, \qquad \delta\bar\eta_\parallel = \frac{1}{16}\frac{1}{8\pi^2}\frac{g^2}{\lambda_\parallel}\log b. \quad (d_T = 2) \tag{3.35}$$

The non-linear contributions to δg can potentially arise from the diagrams in Fig. 3. Explicit computations show that these diagrams generate only higher dimensional terms, and a correction to δg is absent [1].

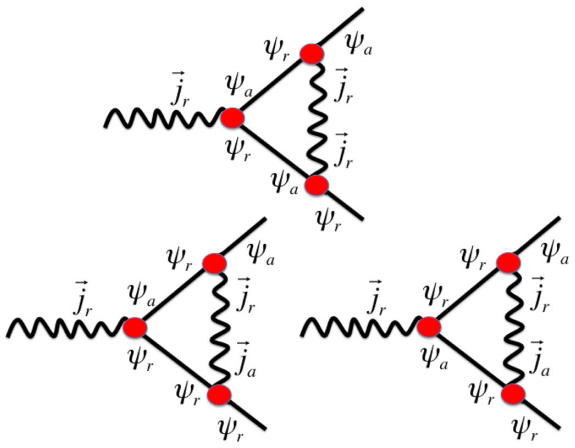

FIG. 3. The real-time diagrams that are relevant for δg. It turns out that there is no correction to δg from these diagrams.

In summary of all these, the renormalization group equations are

$$\frac{d\lambda_\parallel}{d\log b} = (z-4+\eta)\lambda_\parallel + \frac{g^2}{(2\pi)^4}\int d\Omega F(\Omega,\bar\eta_\perp,\bar\eta_\parallel),$$
$$\frac{d\bar\eta_\perp}{d\log b} = (z-2)\bar\eta_\perp + \frac{1}{4(4-d_T)}\frac{1}{8\pi^2}\frac{g^2}{\lambda_\parallel},$$
$$\frac{d\bar\eta_\parallel}{d\log b} = (z-2)\bar\eta_\parallel + \frac{1}{4(6-d_T)}\frac{1}{8\pi^2}\frac{g^2}{\lambda_\parallel},$$
$$\frac{dg}{d\log b} = (z-3+\epsilon/2)g, \tag{3.36}$$

where the angular function $F(\Omega,\bar\eta_\perp,\bar\eta_\parallel)$ is given in (3.21) and (3.22).

IV. FIXED POINT AND THE CRITICAL EXPONENTS

Following the model H analysis [1,2], we define the two coupling constants,

$$f_\perp \equiv \frac{1}{8\pi^2}\frac{g^2}{\bar\eta_\perp\lambda_\parallel}, \qquad f_\parallel \equiv \frac{1}{8\pi^2}\frac{g^2}{\bar\eta_\parallel\lambda_\parallel}. \tag{4.1}$$

Using these variables, the flow equations (3.36) can be written as

$$\lambda_\parallel' = b^{z-4+\eta}\lambda_\parallel\left(1+\frac{1}{2\pi^2}\int d\Omega F(\Omega,1/f_\perp,1/f_\parallel)\log b\right)$$
$$\approx \lambda_\parallel b^{z-4+\eta+\frac{1}{2\pi^2}\int d\Omega F(\Omega,1/f_\perp,1/f_\parallel)},$$
$$\bar\eta_\perp' = b^{z-2}\bar\eta_\perp\left(1+\frac{1}{4(4-d_T)}f_\perp\log b\right) \approx \bar\eta_\perp b^{z-2+\frac{1}{4(4-d_T)}f_\perp},$$
$$\bar\eta_\parallel' = b^{z-2}\bar\eta_\parallel\left(1+\frac{1}{4(6-d_T)}f_\parallel\log b\right) \approx \bar\eta_\parallel b^{z-2+\frac{1}{4(6-d_T)}f_\parallel},$$
$$g' = b^{z-3+\epsilon/2}g, \tag{4.2}$$

where the primed parameters are the renormalized ones after performing one step of integrating a momentum shell and rescaling, and the front factors of b are from naive dimensional scaling, which should be undone for the physical parameters measured in the original coordinate-time. Therefore the physical parameters receive contributions only from the nonlinear effects. We see that these effects are given solely by the parameters $f_\perp$ and $f_\parallel$. More explicitly, for infinitesimal $\log b$,

$$\lambda_\parallel^{\rm phys} = \lambda_\parallel^0 \exp\left[\frac{1}{2\pi^2}\int_0^{\log(\Lambda\xi)} d\log b \times \int d\Omega F(\Omega, 1/f_\perp(\log b), 1/f_\parallel(\log b))\right],$$
$$\bar\eta_\perp^{\rm phys} = \bar\eta_\perp^0 \exp\left[\frac{1}{4(4-d_T)}\int_0^{\log(\Lambda\xi)} d\log b f_\perp(\log b)\right],$$
$$\bar\eta_\parallel^{\rm phys} = \bar\eta_\parallel^0 \exp\left[\frac{1}{4(6-d_T)}\int_0^{\log(\Lambda\xi)} d\log b f_\parallel(\log b)\right], \quad (4.3)$$

where $\lambda_\parallel^0$, $\bar\eta_{\perp,\parallel}^0$ are the parameters at the cutoff Λ in the original theory, and $f_{\perp,\parallel}(\log b)$ are the running couplings by solving the flow equations (3.36). If there exists an attractive fixed point for $f_{\perp,\parallel}$ as we will see shortly, the integral is dominated by the fixed point value for a large $\Lambda\xi \gg 1$ in a scaling regime. This motivates us to look at the flow equations for $f_{\perp,\parallel}$. From (3.36), we obtain

$$\frac{df_\perp}{d\log b} = (\epsilon-\eta)f_\perp - \frac{1}{4(4-d_T)}f_\perp^2 - f_\perp\frac{1}{2\pi^2}\int d\Omega F(\Omega, 1/f_\perp, 1/f_\parallel),$$
$$\frac{df_\parallel}{d\log b} = (\epsilon-\eta)f_\perp - \frac{1}{4(6-d_T)}f_\parallel^2 - f_\parallel\frac{1}{2\pi^2}\int d\Omega F(\Omega, 1/f_\perp, 1/f_\parallel). \quad (4.4)$$

It is not difficult to find a fixed point $(f_\perp^*, f_\parallel^*)$ that makes the right-hand side of the above equations vanish. We consider the leading order in ϵ, i.e., we neglect $\eta \sim \epsilon^2$. First we define a constant C by

$$C\epsilon = \frac{1}{2\pi^2}\int d\Omega F(\Omega, 1/f_\perp^*, 1/f_\parallel^*), \quad (4.5)$$

then the fixed point values are

$$f_\perp^* = 4(4-d_T)(1-C)\epsilon, \quad f_\parallel^* = 4(6-d_T)(1-C)\epsilon, \quad (4.6)$$

and inserting these back to (4.5) gives a self-consistent equation for C,

$$C = \frac{1}{2\pi^2}\int d\Omega F\left(\Omega, \frac{1}{4(4-d_T)}, \frac{1}{4(6-d_T)}\right)(1-C), \quad (4.7)$$

that is,

$$C = \frac{\frac{1}{2\pi^2}\int d\Omega F(\Omega, \frac{1}{4(4-d_T)}, \frac{1}{4(6-d_T)})}{1+\frac{1}{2\pi^2}\int d\Omega F(\Omega, \frac{1}{4(4-d_T)}, \frac{1}{4(6-d_T)})}. \quad (4.8)$$

With the expression for $F(\Omega, x, y)$ in (3.21) and (3.22), we obtain

$$C \approx 0.921 \quad (d_T = 1), \qquad C \approx 0.847 \quad (d_T = 2). \quad (4.9)$$

Once we find the fixed point, the physical parameters are obtained by integrating (4.3) as

$$\lambda_\parallel^{\rm phys} = \lambda_\parallel^0(\Lambda\xi)^{C\epsilon},$$
$$\bar\eta_\perp^{\rm phys} = \bar\eta_\perp^0(\Lambda\xi)^{f_\perp^*/4(4-d_T)} = \bar\eta_\perp^0(\Lambda\xi)^{(1-C)\epsilon},$$
$$\bar\eta_\parallel^{\rm phys} = \bar\eta_\parallel^0(\Lambda\xi)^{f_\parallel^*/4(6-d_T)} = \bar\eta_\parallel^0(\Lambda\xi)^{(1-C)\epsilon}. \quad (4.10)$$

We find that $\bar\eta_\perp$ and $\bar\eta_\parallel$ share the same critical behavior, and this justifies why we need to keep both. The critical exponents x_λ and $x_{\bar\eta}$ are defined by

$$\lambda_\parallel^{\rm phys} \sim \xi^{x_\lambda}, \qquad \bar\eta_{\perp,\parallel} \sim \xi^{x_{\bar\eta}}, \quad (4.11)$$

and we have up to order ϵ,

$$x_\lambda = C\epsilon, \qquad x_{\bar\eta} = (1-C)\epsilon, \quad (4.12)$$

which satisfies the well-known scaling relation in the model H; $x_\lambda + x_{\bar\eta} = \epsilon - \eta$ [1,2]. For a comparison, the original model H has the value $C = 18/19 \approx 0.947$. We find that $d_T = 1$ case is somewhat close to the original model H, but for $d_T = 2$ case the difference in C is about 10% which is significant. We recall that $d_T = 2$ case is relevant for the QCD critical point in a background magnetic field. It is also easy to see that $\bar\eta_{\perp,\parallel}$ grows much faster than $\lambda_\parallel$, which justifies the approximation in obtaining the equation (3.15).

The relaxation frequency for the charge diffusion mode in hydroregime $k \ll \xi^{-1}$ is given by

$$\omega \sim \frac{1}{\chi}\lambda_\parallel^{\rm phys} k_\parallel^2, \quad (4.13)$$

where $\chi \sim \xi^{2-\eta}$ is the susceptibility that is the inverse of the parameter $r^{\rm phys}$. Matching to the critical regime near $k \sim \xi^{-1}$, we have up to order ϵ

$$\omega \sim k^{4-x_\lambda}, \quad (4.14)$$

as the relaxation frequency in the scaling regime $k \gg \xi^{-1}$. For the shear modes, we instead have

$$\omega \sim \bar\eta k^2 \sim k^{2-x_{\bar\eta}}. \quad (4.15)$$

Since the charge diffusion modes relax more slowly than the shear modes, they define the critical slowing down. This gives the dynamic critical exponent [1,2]

$$z = 4 - x_\lambda = 4 - C\epsilon. \quad (4.16)$$

With this, the flow equation for $\lambda_\parallel$ in (3.36) has a finite fixed point for $\lambda_\parallel^* < \infty$. For $d_T = 2$ case, we have $z \approx 3.15$

when $\epsilon = 1$ (three dimensions). This is notably larger than the original model H value, $z \approx 3.05$.

V. CONCLUSION

In this work, we study a variation of dynamic universality class of model H that is obtained by frustrating momentum diffusion and charge current along $d_T = 1$ or $d_T = 2$ spatial dimensions, using the ϵ-expansion. Our main result is the computation of several dynamic critical exponents, such as z. The value of z is particularly important in real-time simulations of critical cumulants in the quark-gluon plasma fireball created in relativistic heavy-ion collision experiments in RHIC [12], whose time-trajectory may pass nearby the QCD critical point and thus may give experimental signatures of QCD critical point fluctuations. This is because z governs the relaxation time scales of critical fluctuations that are driven off-equilibrium by expanding geometry of the plasma. Our result of z taking into account the presence of magnetic field in the heavy-ion collisions should be helpful in improving theoretical predictions of the expected signature of QCD critical point from the heavy-ion collisions experiments planned in the beam-energy scan program at RHIC in the 2018 run.

Comparing the original model H ($d_T = 0$), the case of $d_T = 1$ and $d_T = 2$, we clearly see the trend that the constant C defined in Sec. IV decreases as d_T increases (that is, $C = 0.947, 0.921$ and 0.847 respectively), resulting in an increase of z as d_T increases. From the relation $x_\lambda = C\epsilon$, we see that the strength of C represents how strongly the non-linear coupling affects the divergence of the conductivity. Having larger d_T clearly reduces more the available phase space for fluctuations that contribute to the non-linear effects, and this could explain the observed dependence of C, and hence z, on d_T.

As a further direction, one could try to compute other refined quantities in these models such as scaling functions. It should also be possible to go to a next order in ϵ-expansion using the method in Ref. [18].

ACKNOWLEDGMENTS

We thank Rob Pisarski, Misha Stephanov, and Ismail Zahed for discussions. This work is supported by the U.S. Department of Energy, Office of Science, Office of Nuclear Physics, Grant No. DE-SC0018209, and within the framework of the Beam Energy Scan Theory (BEST) Topical Collaboration.

[1] E. D. Siggia, B. I. Halperin, and P. C. Hohenberg, Renormalization-group treatment of the critical dynamics of the binary-fluid and gas-liquid transitions, Phys. Rev. B **13**, 2110 (1976).
[2] P. C. Hohenberg and B. I. Halperin, Theory of dynamic critical phenomena, Rev. Mod. Phys. **49**, 435 (1977).
[3] L. P. Kadanoff and J. Swift, Transport coefficients near the liquid-gas critical point, Phys. Rev. **166**, 89 (1968).
[4] K. Kawasaki, Kinetic equations and time correlation functions of critical fluctuations, Ann. Phys. (N.Y.) **61**, 1 (1970).
[5] K. G. Wilson and M. E. Fisher, Critical Exponents in 3.99 Dimensions, Phys. Rev. Lett. **28**, 240 (1972).
[6] K. G. Wilson and J. B. Kogut, The renormalization group and the epsilon-expansion, Phys. Rep. **12**, 75 (1974).
[7] M. A. Stephanov, K. Rajagopal, and E. V. Shuryak, Event-by-event fluctuations in heavy ion collisions and the QCD critical point, Phys. Rev. D **60**, 114028 (1999).
[8] B. Berdnikov and K. Rajagopal, Slowing out-of-equilibrium near the QCD critical point, Phys. Rev. D **61**, 105017 (2000).
[9] D. T. Son and M. A. Stephanov, Dynamic universality class of the QCD critical point, Phys. Rev. D **70**, 056001 (2004).
[10] L. Adamczyk *et al.* (STAR Collaboration), Energy Dependence of Moments of Net-proton Multiplicity Distributions at RHIC, Phys. Rev. Lett. **112**, 032302 (2014).
[11] M. A. Stephanov, On the Sign of Kurtosis near the QCD Critical Point, Phys. Rev. Lett. **107**, 052301 (2011).
[12] S. Mukherjee, R. Venugopalan, and Y. Yin, Real time evolution of non-Gaussian cumulants in the QCD critical regime, Phys. Rev. C **92**, 034912 (2015).
[13] A. Bzdak and V. Skokov, Event-by-event fluctuations of magnetic and electric fields in heavy ion collisions, Phys. Lett. B **710**, 171 (2012).
[14] W. T. Deng and X. G. Huang, Event-by-event generation of electromagnetic fields in heavy-ion collisions, Phys. Rev. C **85**, 044907 (2012).
[15] K. Tuchin, Time and space dependence of the electromagnetic field in relativistic heavy-ion collisions, Phys. Rev. C **88**, 024911 (2013).
[16] L. McLerran and V. Skokov, Comments about the electromagnetic field in heavy-ion collisions, Nucl. Phys. **A929**, 184 (2014).
[17] S. Li and H. U. Yee, Shear viscosity of quark-gluon plasma in weak magnetic field in perturbative QCD: Leading log, arXiv:1707.00795.
[18] K. G. Wilson, Feynman Graph Expansion for Critical Exponents, Phys. Rev. Lett. **28**, 548 (1972).